Anal. Bioanal. Electrochem., Vol. 14, No. 5, 2022, 455-469

Analytical & Bioanalytical Electrochemistry

2022 by CEE
www.abechem.com

Full Paper

Plasmon Enhanced Electrooxidation of Ethanol using A New Au-Pt/TiO_2/MWCNTs Photoelectrocatalyst

Farah Al-Hammashi, Behjat Deiminiat, and Gholam Hossein Rounaghi*

Department of Chemistry, Faculty of Sciences, Ferdowsi University of Mashhad, Mashhad, Iran

*Corresponding Author, Tel.: +985138805542

E-Mails: ghrounaghi@yahoo.com; ronaghi@um.ac.ir

Received: 18 August 2021 / Received in revised form: 15 April 2022 / Accepted: 19 April 2022 / Published online: 31 May 2022

Abstract- A novel photoelectrocatalyst composed from multiwalled carbon nanotubes (MWCNTs), titanium dioxide (TiO_2) and gold-platinum bimetallic nanoparticles (Au–PtNPs) was prepared on the surface of a fluorine-tin oxide (FTO) electrode and it was used for electrooxidation of ethanol molecules. Multiwalled carbon nanotubes were utilized as the catalyst support to improve the electrical transmission. The TiO_2 nanoparticles were transferred onto the surface of MWCNTs/FTO modified electrode and then, the surface of the electrode was coated with gold-platinum nanoparticles. The surface morphology and chemical composition of the prepared Au-Pt/TiO_2/MWCNTs photoelectrocatalyst were characterized using scanning electron microscopy (SEM) and energy dispersive X-ray (EDX) spectroscopy. The fabrication process of the photoelectrocatalyst was investigated by cyclic voltammetry and chronoamperometry techniques. The exchange current densities (J_0) were calculated for Pt/FTO, Pt/MWCNTs/FTO, Pt/TiO_2/MWCNTs/FTO and Au-Pt/TiO_2/MWCNT/FTO electrodes and they were found to be: 4.10×10^{-5}, 6.06×10^{-5}, 1.45×10^{-4} and 1.89×10^{-4} mA cm^{-2}, respectively. Also, the values of J_0 for Pt/TiO_2/MWCNTs/FTO and Au-Pt/TiO_2/MWCNTs/FTO in the presence of light were obtained 2.0×10^{-4} and 5.1×10^{-4} mA cm^{-2}, respectively. The obtained results reveal that the Au-Pt/TiO_2/MWCNTs/FTO electrode has the higher J_0 value in the presence of UV-Vis light and the light irradiation can accelerate the ethanol oxidation process. The experimental results showed that the proposed photoelectrocatalyst has an excellent catalytic activity for oxidation of ethanol molecules under the UV-Vis light irradiation which is due to the synergistic effect between the TiO_2 photocatalyst and gold-platinum electrocatalyst.

Keywords- Photoelectrocatalyst; Multiwalled carbon nanotubes; Titanium dioxide; Gold-platinum nanoparticles; Fluorine-tin oxide; Electrooxidation of ethanol

1. INTRODUCTION

Fuel cells are one of the most important candidates for the production of clean energy with high efficiency [1]. Ethanol is a promising fuel for application in direct alcohol fuel cells (DAFCs) due to its high energy density, abundance, easy-storage and low toxicity [2,3]. However, ethanol has a C-C bond and the complete electrooxidation of ethanol to CO_2 is slow and it involves the transference of 12 electrons in the anodic reaction and formation of many adsorbed intermediates [4,5]. Therefore, it is necessary to accelerate the anodic reaction by using electrocatalysts. Platinum is commonly used as a powerful electrocatalyst for electrooxidation of ethanol in direct ethanol fuel cells (DEFCs) because it is active and stable in acidic media. But platinum is easily poisoned by the strongly adsorbed intermediates such as CO coming from the dissociation of ethanol molecules. Also, it is very expensive and therefore, it is not affordable for industrial applications [6,7]. In order to overcome these problems, platinum distributed on the carbon support is usually applied as the anode catalyst. Since the electrocatalytic oxidation process of the ethanol molecules is a superficial effect, the electrocatalyst should have a highest surface area. Distributing the platinum nanoparticles on a conductive, porous and non-precious support like carbon nanotubes, increases the surface area and also provides the higher tolerance to CO and the other intermediates which are produced at the surface of the catalyst [4,8,9]. Another way for improving the catalytic activity of the Pt-based catalysts, is the alloying the Pt nanoparticles with a second or third component such as Sn, Au, Os, Co, Pd, Ru, Rh and Cu metallic elements [10-18]. The good performance of the binary and ternary Pt-based catalysts can be attributed to the bi-functional mechanism. In this mechanism, electrooxidation of ethanol molecules occurs on the platinum active sites and the additional metal, dissociates the water molecules into OH and H groups at a lower potential compared to the pure platinum. Then, the surface OH groups oxidize the strongly adsorbed CO to CO_2 and the platinum surface becomes active [19,20].

Another strategy for enhancing the electrocatalytic performance of Pt, is to prepare a catalyst through the coupling of platinum with photoactive semiconductors [21-23]. In such system, light irradiation excites the semiconductor which results in the generation of the electron-hole pairs and oxidation of ethanol molecules. In this case, the ethanol molecules are oxidized by synergistic electrocatalytic and photocatalytic reactions, and the currents which are produced from both phenomena are combined and, therefore, the oxidation performance of the ethanol molecules is increased. On the other hand, the light illumination prevents the platinum deactivation during the ethanol electrooxidation through the desorption of CO from the Pt surface [24].

Recently, TiO_2 has attracted great attention as a photoactive material due to its high surface area, non-toxicity, low cost, and excellent photocatalytic activity [25]. However, TiO_2 has a large band gap (about 3.2 eV) and it shows photocatalytic activity only under UV irradiation which limits its broad application [26]. Also, the photogenerated electron-hole pairs tend to

recombine rapidly at the surface of TiO_2 which decreases the photocatalytic efficiency. Therefore, it is important to develop new catalysts with the desired structure and optical properties. The most effective way in this field is the combination of TiO_2 with metallic elements like Pt and Au and also non-metallic elements such as C and N.

In this study, a new photoelectrocatalyst was prepared through layer-by-layer modification of f-MWCNTs, TiO_2 and Au–PtNPs on the surface of the FTO electrodes. These layers were investigated by scanning electron microscopy (SEM) and energy-dispersive X-ray spectroscopy (EDX). Cyclic voltammetry and chronoamperometry techniques were used to characterize the catalytic performance of the prepared layers for oxidation of ethanol molecules in acidic solutions.

2. EXPERIMENTAL

2.1. Chemicals

All chemicals used in this research project, were of analytical grade. Ethanol, hexachloro platinic acid hexahydrate ($H_2PtCl_6.6H_2O$), perchloric acid ($HClO_4$) and sulfuric acid (H_2SO_4) were purchased from Merck (Darmstadt, Germany). Tetrachloroauric acid trihydrate ($HAuCl_4.3H_2O$) and titanium oxide (TiO_2) were obtained from Sigma-Aldrich chemical company. Multiwalled carbon nanotubes (purity >95%, outer diameter 5–15 nm) were purchased from US research nanomaterials (Houston, USA). Deionized water was used for the preparation of solutions throughout the work.

2.2. Instrumentation

The electrochemical and photoelectrochemical studies were performed with a μ Autolab potentiostat/galvanostat Type III (Netherlands). All the experiments were carried out in a three-electrode cell. A modified FTO electrode (Solaronix, Switzerland) was used as the working electrode and a platinum wire (Metrohm, Netherlands) and an Ag/AgCl electrode (Azar electrode, Iran) were employed as the counter and reference electrodes, respectively. A Xe lamp (150 W) was used as the light source. The SEM images of the photoelectrocatalyst at different construction steps were taken by a LEO 1450 VP scanning electron microscope (Germany). The surface elemental analysis of the catalyst was performed using an energy dispersive X-ray (EDX) microanalyzer model Oxford-7353.

2.3. Preparation of Au-Pt/TiO_2/ MWCNTs photoelectrocatalyst

The Au-Pt/TiO_2/MWCNTs photoelectrocatalyst was prepared at the surface of the FTO substrate. To this end, the FTO glass plates were cut into 20×5 mm^2 pieces and then cleaned in a solution containing deionized water and soap under sonication for 10 min. After that, the FTO pieces were sonicated sequentially for 5 min in isopropanol, 5 min in ethanol and 2 min

in acetone. The MWCNTs suspension was prepared by dispersing 1.0 mg of f-MWCNTs in 1.0 mL of dimethylformamide (DMF) under sonication for 10 min. 20 μL of the prepared suspension was transferred onto the surface of a FTO electrode (with a surface area of 0.25 cm^2) and allowed to dry under an infrared lamp. In the next step, 1.0 mg of TiO_2 powder was sonicated in 1.0 mL deionized water for 15 min and then, 25 μL aliquot of the suspension was dropped on the surface of MWCNTs/FTO modified electrode and the solvent was evaporated under the IR lamp. Finally, the Au-Pt nanoparticles were deposited at the surface of TiO_2/MWCNTs/FTO electrode from a $HClO_4$ 0.2 M solution containing $HAuCl_4.3H_2O$ 1 mM and $H_2PtCl_6.3H_2O$ 2 mM by applying the potential in the range of −0.4 to +1.2 V for 12 cycles with a scan rate of 50 mV s^{-1}. For comparison, the Pt/FTO, Pt/MWCNTs/FTO and Pt/TiO_2/MWCNTs/FTO catalysts were prepared under the same conditions.

2.4. Characterization of Au-Pt/ TiO_2/ MWCNTs photoelectrocatalyst

Scanning electron microscopy (SEM) was used to investigate the surface morphology of the Au-Pt/TiO_2/MWCNTs photoelectrocatalyst at different construction stages. Figure 1A, shows a uniform and spongy surface for the bare FTO electrode and Figure 1B, depicts the curved tubular structures of MWCNTs. Figure 1C, illustrates the globular shaped TiO_2 nanoparticles at the surface of MWCNTs/FTO. Figure 1D, displays the homogeneous dispersion of Au–Pt nanoparticles with spherical morphology after co-electrodeposition.

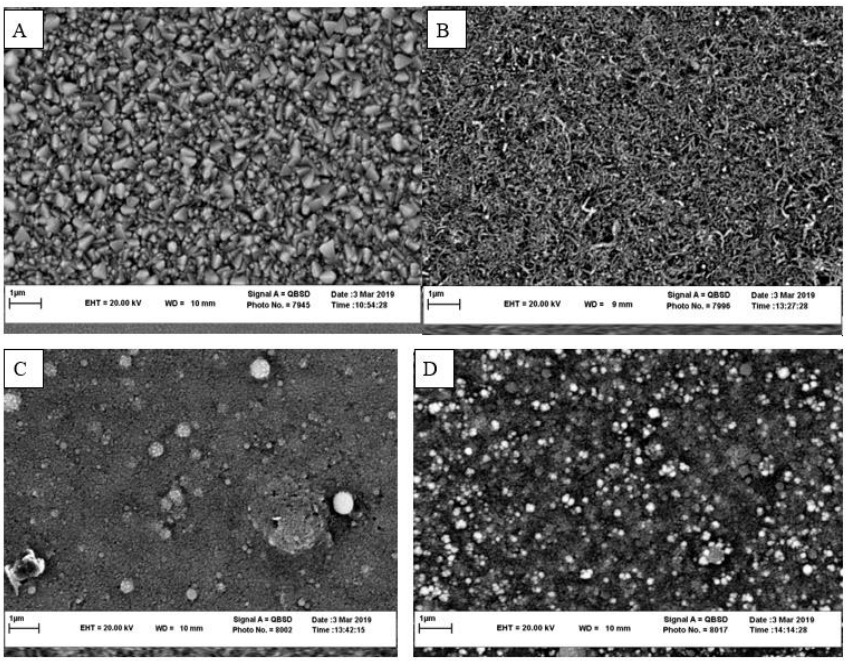

Figure 1. The SEM images of the (A) bare FTO, (B) MWCNTs/FTO, (C) TiO_2/MWCNTs /FTO and (D) Au–Pt /TiO_2/MWCNTs/FTO

For further evaluation, the surface elemental analysis of the photoelectrocatalyst was performed by energy dispersive X-ray (EDX) technique. The EDX spectrum of the bare FTO electrode (Figure 2A) indicates the presence of Sn, Si and O elements. The C peak in Figure 2B can be attributed to the presence of MWCNTs at the FTO surface. Figure 2C, shows the EDX spectrum of TiO_2/MWCNTs/FTO. The Ti peaks are clearly seen in this Figure which confirms the successful immobilization of TiO_2 nanoparticles on the surface of MWCNTs/FTO. The results obtained from the EDX analysis of Au-Pt/TiO_2/MWCNTs/FTO (Figure 2D), show that the Au–Pt nanoparticles have been successfully deposited on the surface of TiO_2/MWCNTs modified FTO electrode.

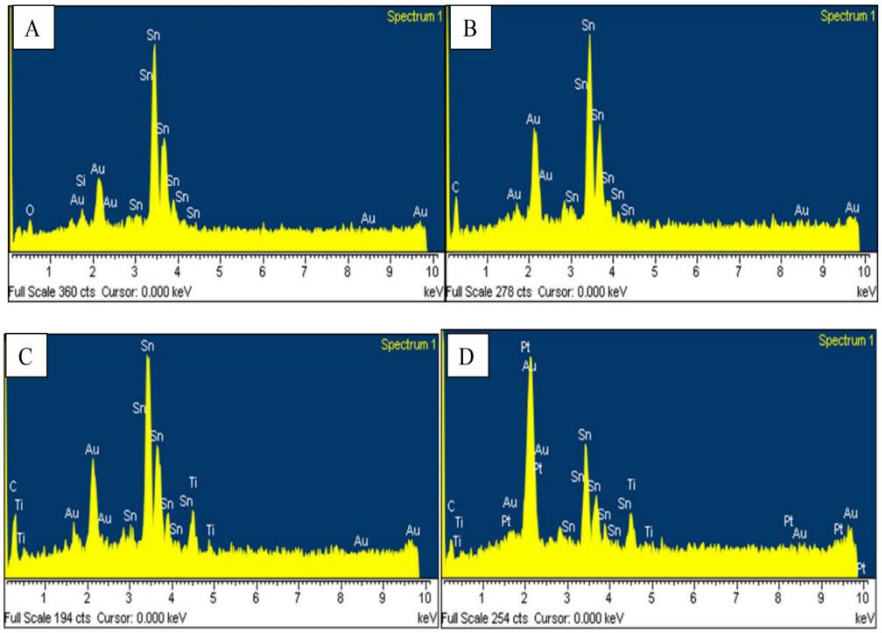

Figure 2. The EDX spectra of the (A) bare FTO, (B) MWCNTs/FTO, (C) TiO_2/MWCNTs /FTO and (D) Au–Pt/TiO_2/MWCNTs/FTO

In order to further support the results obtained from SEM and EDX studies, the XRD pattern of the Au-Pt/TiO_2/MWCNTs/FTO was also recorded (Figure 3A). The sharp peaks which are appeared at 21.5° and 23.8° can be attributed to the diffraction planes of TiO_2 nanoparticles [27]. The peak at 26.5° is indexed as (002) and it can be assigned to the MWCNTs [28]. FTO shows three diffraction peaks at 33.7°, 37.7° and 51.6° [29]. Three diffraction peaks which are seen at 37.8°, 44.6° and 65.5° can be attributed to the Au and Pt nanoparticles [28,30].

Figures 3B and 3C, show the XPS spectra of the Au-Pt/TiO_2/MWCNTs/FTO surface. These Figures confirms the existence of the O, Ti, C, Pt, and Au elements in the surface of the photoelectrode.

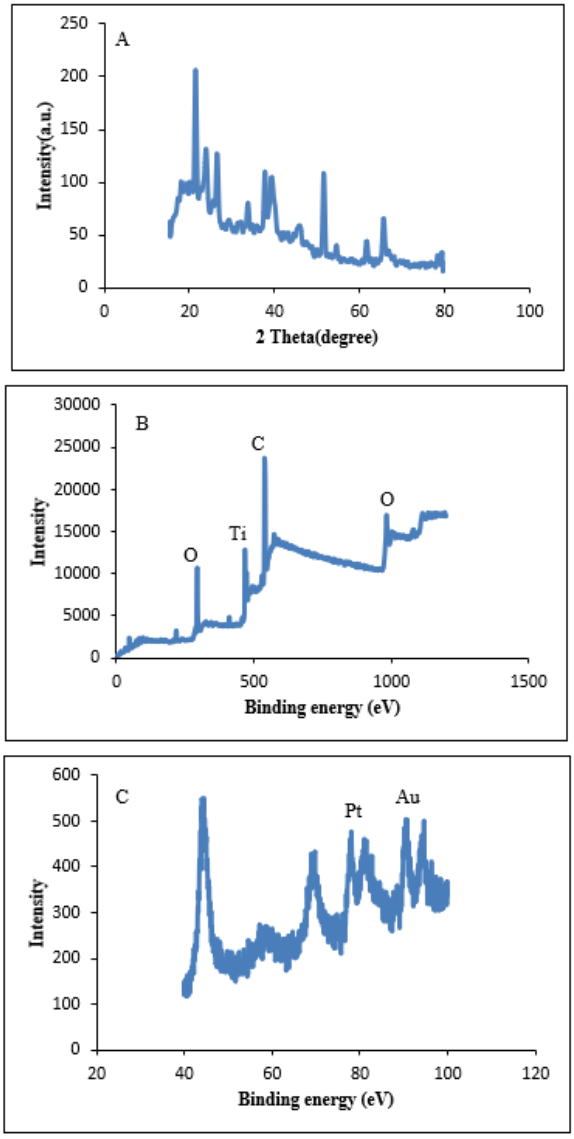

Figure 3. (A) XRD pattern of Au-Pt/TiO_2/MWCNTs/FTO, (B) XPS spectrum of Au-Pt/TiO_2/MWCNTs/FTO surface and (C) the initial part (20-120 eV) of the XPS spectrum of Au-Pt/TiO_2/MWCNTs/FTO with high resolution

3. RESULTS AND DISCUSSION

3.1. Electrooxidation of ethanol

Electrooxidation of ethanol molecules at the surface of Au-Pt/TiO_2/MWCNTs photoelectrocatalyst was investigated using cyclic voltammetry technique. Figure 4, shows the corresponding voltammogram in a $HClO_4$ 0.3 M solution containing ethanol 0.7 M at the potential range of 0 to 1.5 V and scan rate of 50 mV s^{-1}. As is evident in this Figure, when the potential sweep is initiated in the anodic direction, the dissociative adsorption of ethanol molecules is happened (region I) which results in the formation of the CO species [31]. By sweeping toward more positive potentials, two oxidation peaks are found at around 0.75 V and

1.15 V due to the formation of the CO_2 (region II) and acetaldehyde (region III) species, respectively [32,33]. At the higher potentials, the decay of the second oxidation peak is occurred which can be attributed to the decrease of the adsorption sites at the catalyst surface due to the oxidation of platinum (region IV) [34].

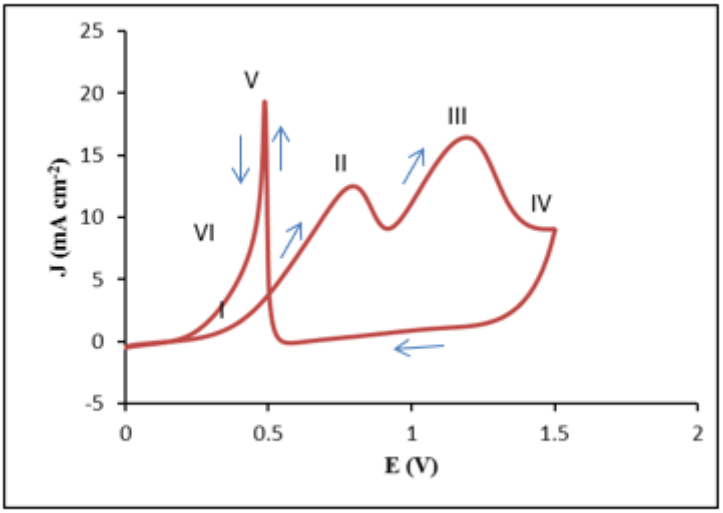

Figure 4. Cyclic voltammogram (CV) of ethanol oxidation under the light illumination at the surface of Au–Pt/TiO_2/ MWCNTs/FTO photoelectrocatalyst in 0.3 M $HClO_4$ containing 0.7 M ethanol at a scan rate of 50 mV s^{-1}

In the reverse sweep, the reduction of the platinum oxide to platinum occurs and the active sites are produced at the surface of the catalyst. It should be mentioned that the absence of the platinum oxide reduction peak is due to the presence of an oxide layer on the electrode surface. This oxide layer prevents the formation of the organic radical and inhibits the occurrence of an electrochemical peak [35]. But, as soon as the reduction of platinum oxide takes place, the re-oxidation of ethanol molecules and intermediate species such as Pt–OCH_2CH_3, Pt–CHOH–CH_3 $(Pt)_2$=COH–CH_3, Pt–$COCH_3$ and Pt–C=O, which are formed from the incomplete oxidation of ethanol molecules in the forward step, is carried out and, therefore, a backward anodic peak is observed in the cyclic voltammogram (region V) [36]. At the more negative potentials, the intermediate species are hardly oxidized at such low potentials which leads to the poisoning of the photoelectrocatalyst (region VI) [37].

The catalytic behavior of Pt, Pt/MWCNTs, Pt/TiO_2/MWCNTs and Au-Pt/TiO_2/MWCNTs catalysts for electrooxidation of ethanol molecules was characterized by cyclic voltammetry and the corresponding results are depicted in Figure 5. As can be seen in Figure 5, all the prepared catalysts are active for the electrooxidation process of ethanol molecules. However, the Au-Pt/TiO_2/MWCNTs photoelectrocatalyst has the greater catalytic performance than the other catalysts and the current density is improved under UV-Vis light illumination. The better

performance of the Au-Pt/TiO_2/MWCNTs photoelectrocatalyst can be assigned to the presence of MWCNTs layer, TiO_2 nanoparticles and Au-Pt bimetallic alloy in the catalyst composition and the synergistic effect between the Au-Pt bimetallic electrocatalyst and TiO_2 photocatalyst.

Pt/FTO has only platinum as the electrocatalyst which is easily poisoned by the CO intermediate and, therefore, the electrode performance is decreased. The presence of Au along with Pt in the composition of the catalyst, improves the current density and also decreases the poisoning of the electrode surface by the oxidation of intermediates through the bi-functional mechanism. In this mechanism, adsorption of the ethanol molecules onto the platinum sites results in the formation of the adsorbed intermediate COads and the additional metal dissociates the water molecules into OH and H groups. Then, the COads reacts with the OH which is adsorbed at Au surface, to yield the CO_2 molecules.

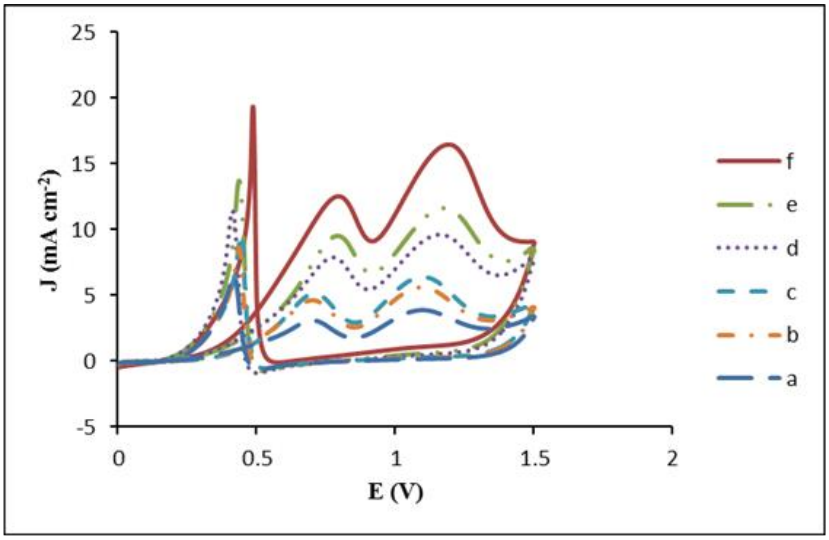

Figure 5. Cyclic voltammograms (CVs) of ethanol oxidation at the surface of (a) Pt/FTO, (b) Pt/MWCNTs/FTO, (c) Pt/TiO_2/MWCNTs/FTO, (d) Au–Pt/TiO_2/MWCNTs/FTO in the absence of light, (e) Pt/TiO_2/MWCNTs/FTO and (f) Au–Pt /TiO_2/MWCNTs/FTO in the presence of light in 0.3 M $HClO_4$ containing 0.7 M ethanol at a scan rate of 50 mV s^{-1}

In addition to the electrooxidation process, the photo-oxidation of the ethanol molecules also results in the better performance of the fabricated catalyst. Irradiation of UV-Vis light onto the surface of Au-Pt/TiO_2/MWCNTs photoelectrocatalyst, increases the anodic peak current density of ethanol oxidation. The current density at the surface of Au-Pt/TiO_2/MWCNTs /FTO modified electrode with UV-Vis light illumination is about 1.7 times higher than without the UV-Vis illumination. Irradiation of UV light, promotes the electron from the valence band to the conducting band of TiO_2 molecules and an electron–hole pair is produced on the surface of TiO_2. The photoexcited electron is transferred to the MWCNTs layer and carried away by the

external circuit and then, the ethanol molecules are oxidized by the photogenerated holes ($TiO_2(h^+)$). Moreover, under visible light illumination, the electron-hole pairs are formed in Au nanoparticles due to the surface plasmon resonance phenomenon. The photoexcited electrons are injected into the conduction band of TiO_2 molecules and then conducted away by the external circuit. This electron transfer process, results in a hole-rich surface of Au nanoparticles and improvement the catalytic activity of the electrode toward the electrooxidation of ethanol molecules [21,38,39].

The collaboration between the electrooxidation and photo-oxidation of ethanol molecules can be explained by the involved mechanisms. In the absence of UV-Vis light, the recorded anodic peak current is due to the electrooxidation of ethanol molecules by the platinum and gold catalysts. In the presence of UV-Vis light, the photogenerated holes in the valence band of Au are able to accept the electron from ethanol molecules. The photo-electrooxidation process of ethanol molecules is already known and it has been reported by some researchers [40].

3.2. Electrochemical impedance spectroscopy (EIS) study

Figure 6, shows the Nyquist diagrams of different catalysts for ethanol electrooxidation in 0.3 M $HClO_4$ containing 0.7 M ethanol. As can be seen in this figure, the Au-Pt/TiO_2/MWCNTs has a smaller semicircle under the UV-Vis irradiation compared to the other catalysts which indicates a higher electron transfer resistance (R_{et}) against the oxidation process of ethanol. This behavior can be attributed to the homogenous dispersion of Au and Pt nanoparticles on to the TiO_2/MWCNTs nanocomposite layer and the photogeneration of electron-hole pairs at the surface of Au nanoparticles.

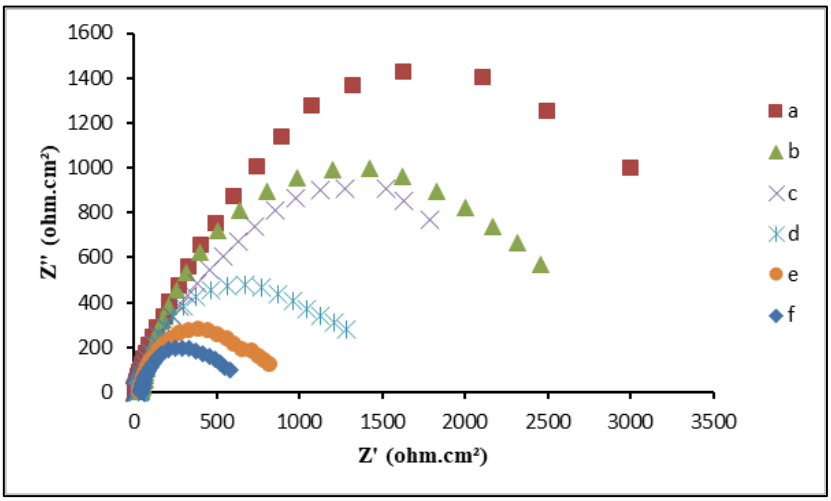

Figure 6. Nyquist plots of (a) Pt/FTO, (b) Pt/MWCNTs/FTO, (c) Pt/TiO_2/MWCNTs/FTO, (d) Au–Pt/TiO_2/MWCNTs/FTO in the absence of light, (e) Pt/TiO_2/MWCNTs/FTO and (f) Au–Pt /TiO_2/MWCNTs/FTO in the presence of light in 0.3 M $HClO_4$ containing 0.7 M ethanol

3.3. Chronoamperometric studies

Chronoamperometry technique was used for the further evaluation of the catalytic performance of the Pt, Pt/MWCNTs, Pt/TiO_2/MWCNTs and Au-Pt/TiO_2/MWCNTs catalysts for oxidation of ethanol in solutions. Figure 7A, shows the current-time curves for these catalysts. As is seen in this Figure, all the catalysts show a decrease in current density due to the formation of intermediates during the ethanol oxidation process. Nevertheless, the current density for oxidation of ethanol molecules on the surface of Au-Pt/TiO_2/MWCNTs catalyst under the light illumination is higher than those obtained for the other catalysts. These results show that the Au-Pt/TiO_2/MWCNTs catalyst has a good stability and poisoning tolerance and, therefore, it is more appropriate for long time operation [41].

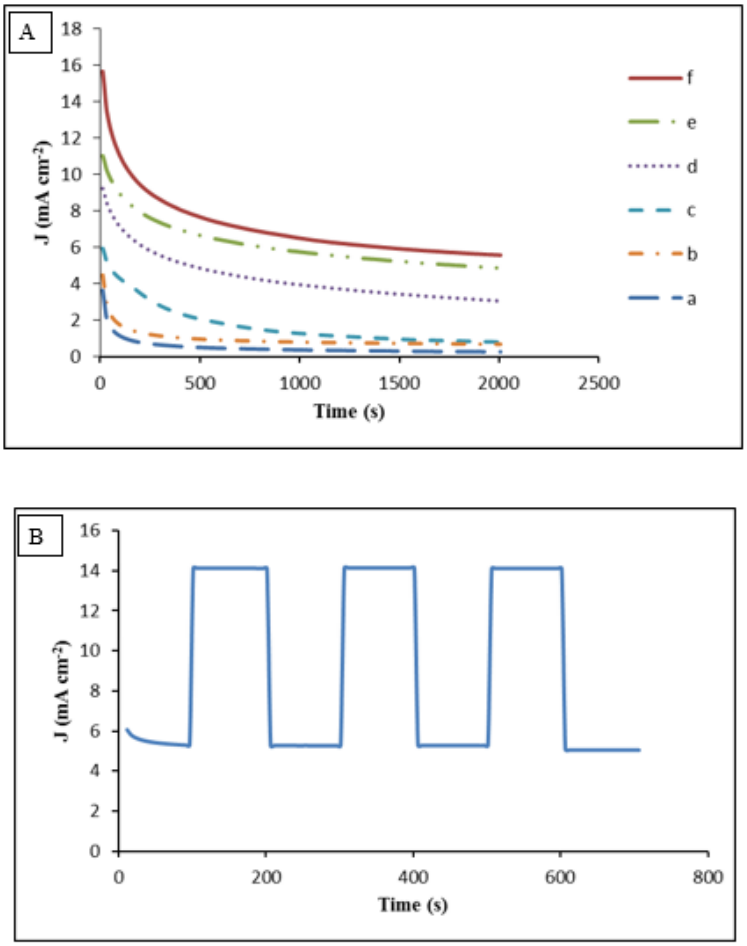

Figure 7. (A) Chronoamperograms of (a) Pt/FTO, (b) Pt/MWCNTs/FTO, (c) Pt /TiO_2/MWCNTs/FTO, (d) Au–Pt/TiO_2/MWCNTs/FTO in the absence of light, (e) Pt /TiO_2/MWCNTs/FTO and (f) Au–Pt/TiO_2 /MWCNTs/FTO in the presence of light in 0.3 M $HClO_4$ containing 0.7 M ethanol and (B) photocurrent responses of Au–Pt/TiO_2/MWCNTs/FTO under pulsating light illumination in 0.3 M $HClO_4$ containing 0.7 M ethanol

The effect of the UV-Vis light illumination on the current density of ethanol oxidation was investigated by chronoamperometry in repeated on-off cycles. Figure 7B, displays the current density at the surface of Au-Pt/TiO_2/MWCNTs photoelectrocatalyst as a function of time by switching the light on-off in a duration of 100 s. As is obvious in this Figure, there is a weak current density in the absence of light. When the light is on, the current density increases instantly and reaches to a steady state. When the light is off, the current density reduces immediately and it comes back to its previous level.

3.4. Kinetic studies

The kinetic studies for the oxidation process of ethanol molecules were performed using the Tafel plots. The Tafel plots are shown in Figure 8. The exchange current densities (J_0) were calculated for Pt/FTO, Pt/MWCNTs/FTO, Pt/TiO_2/MWCNTs/FTO and Au-Pt/TiO_2/MWCNT/FTO electrodes and they were found to be: 4.10×10^{-5}, 6.06×10^{-5}, 1.45×10^{-4} and 1.89×10^{-4} mA cm^{-2}, respectively. Also, the values of J_0 for Pt/TiO_2/MWCNTs/FTO and Au-Pt/TiO_2/MWCNTs/FTO in the presence of light were obtained 2.0×10^{-4} and 5.1×10^{-4} mA cm^{-2}, respectively. The obtained results reveal that the Au-Pt/TiO_2/MWCNTs/FTO electrode has the higher J_0 value in the presence of UV-Vis light and the light irradiation can accelerate the ethanol oxidation process.

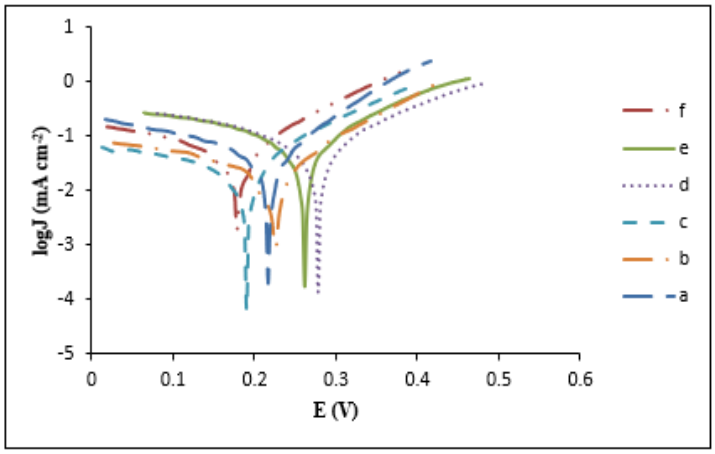

Figure 8. Tafel plots of (a) Pt/FTO, (b) Pt/MWCNTs/FTO, (c) Pt/TiO_2/MWCNTs/FTO, (d) Au–Pt/TiO_2/MWCNTs/FTO in the absence of light, (e) Pt/TiO_2/MWCNTs/FTO and (f) Au–Pt/TiO_2/MWCNTs/FTO in the presence of light

3.5. Effective parameters on the electrooxidation of ethanol

3.5.1. Effect of the amounts of MWCNTs and TiO_2

The influence of the amounts of MWCNTs and TiO_2 on the oxidation peak current density of ethanol molecules was studied. The obtained results are shown in Figures 9A and 9B. As is

evident in these Figures, the anodic peak current densities increase progressively with increasing the volume of MWCNTs suspension up to 20 μL and TiO_2 suspension up to 25 μL and then they decrease. Therefore, these values were selected as the optimum volumes for the preparation of Au-Pt/TiO_2/MWCNTs photoelectrocatalyst. The increase in the current densities may be due to the high electrical conductivity and specific surface area of MWCNTs and also the photocatalytic activity of TiO_2.

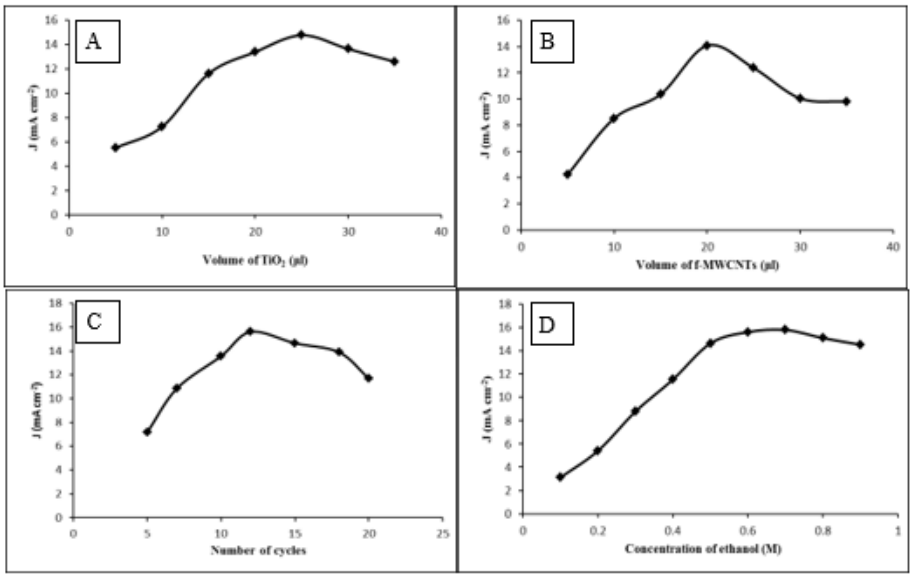

Figure 9. Effect of the (A) amount of MWCNTs, (B) amount of TiO_2, (C) number of electrodeposition cycles of Au–Pt nanoparticles and (D) ethanol concentration on the oxidation peak current density of ethanol

3.5.2. Effect of the number of electrodeposition cycles of Au–Pt nanoparticles

The effect of the number of electrodeposition cycles of Au–Pt nanoparticles on the ethanol oxidation was also investigated and it was optimized. Figure 9C, shows the anodic peak current density at different scan cycles. With increasing the number of scan cycles from 5 to 12, the anodic peak current density increases and reaches a maximum at 12 cycles. Below 12 cycles, the Au–Pt nanoparticles are uniformly deposited at the surface of TiO_2/MWCNTs/FTO which improves the electrocatalytic activity of Au–Pt bimetallic catalyst. It seems that at higher cycles than 12, the formation of agglomerated Au–Pt nanoparticles leads to the decrease of current density.

3.5.3. Effect of ethanol concentration

The ethanol crossover from anode to cathode is an important process which occurs at high concentrations of ethanol and leads to the low efficiency of fuel cells [42]. Therefore, it is necessary to optimize the concentration of ethanol. Figure 9D, shows the changes of the anodic

peak current density with the ethanol concentration. As can be seen in this Figure, the current density increases with increasing the ethanol concentration up to 0.7 M and then it remains almost constant due to the saturation of the active sites at the catalyst surface.

3.6. Catalytic activity of different substrates

In order to obtain an appropriate substrate for the preparation of Au-Pt/TiO_2/MWCNTs photoelectrycatalyst, different electrodes such as glassy carbon, gold, platinum and FTO were tested. Figure 10, shows the cyclic voltammograms of ethanol oxidation at the surface of these electrodes under the same conditions. As is seen in Figure 10, the Au-Pt/TiO_2/MWCNTs/FTO shows a higher catalytic activity compared to the other electrode surfaces used in this study which can be attributed to the transparency of the FTO substrate. Therefore, FTO was selected as the substrate for immobilization of the MWCNTs and TiO_2 layers and Au-Pt nanoparticles.

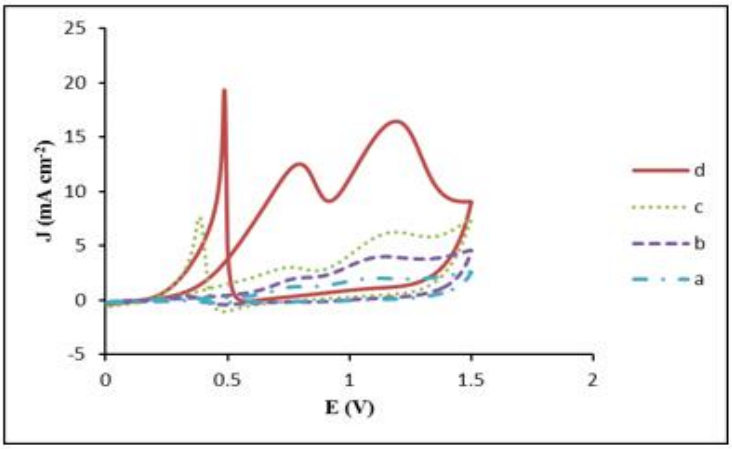

Figure 10. Comparison of the anodic peak current density for ethanol oxidation at the surface of (a) Au–Pt /TiO_2/MWCNTs/GCE, (b) Au–Pt /TiO_2/MWCNTs/AuE, (c) Au–Pt /TiO_2/ MWCNTs/PtE and (d) Au–Pt /TiO_2/MWCNTs/FTO

4. CONCLUSION

The purpose of the present study, is the preparation of a new anodic photoelectrocatalyst for the oxidation of ethanol molecules in direct ethanol fuel cells. The FTO glass slices were modified by MWCNTs and TiO_2 films and Au-Pt nanoparticles, respectively, and they were characterized using scanning electron microscopy (SEM) and energy dispersive X-ray (EDX) spectroscopy. The electrochemical studies demonstrated that the prepared Au-Pt/TiO_2/ MWCNTs photoelectrycatalyst has an excellent performance for electrooxidation of ethanol molecules under the light illumination of UV-Vis in comparison with the other catalysts used in this study. It seems that this better catalytic activity is due to the synergistic effect between the Au-Pt bimetallic electrocatalyst and TiO_2 photocatalyst. Moreover, the Tafel plots showed

that the electrooxidation of ethanol molecules at Au-Pt/TiO_2/MWCNTs/FTO surface is easier from the kinetic viewpoint than the other prepared catalysts.

Acknowledgments

The authors gratefully acknowledge the support of this research work by Ferdowsi University of Mashhad, Mashhad, Iran (Grant No. 3.50163).

REFERENCES

[1] B. Liu, J. H. Chen, X. X. Zhong, K. Z. Cui, H. H. Zhou, and Y. F. Kuang, J. Colloid Interface Sci. 307 (2007) 139.
[2] Y. Oh, J. Kang, S. Nam, S. Byun, and B. Park, Mater. Chem. Phys. 135 (2012) 188.
[3] M. F. Silva, B. C. Batista, E. Boscheto, H. Varela, and G. A. Camara, J. Brazilian Chem. Soc. 23 (2012) 831.
[4] P. dos Santos Correa, E. L. da Silva, R. F. da Silva, C. Radtke, B. Moreno, E. Chinarro, and C. de Fraga Malfatti, Int. J. Hydrogen Energy 37 (2012) 9314.
[5] I. Razavipanah, G. H. Rounaghi, and M. H. Zavvar, J. Iranian Chem. Soc. 10 (2013) 1279.
[6] R. G. Freitas, L. F. Marchesi, M. R. Forim, L. O. Bulhões, E. C. Pereira, M. C. Santos, and R. T. Oliveira, J. Brazilian Chem. Soc. 22 (2011) 1709.
[7] Q. Y. Qian, C. Yang, Y. G. Zhou, S. Yang, and X. H. Xia, J. Electroanal. Chem. 660 (2011) 57.
[8] D. J. Guo, J. Power Sources 196 (2011) 679.
[9] Z. Jiang, Z. J. Jiang, and Y. Meng, Appl. Surf. Sci. 257 (2011) 2923.
[10] W. T. Kuang, Z. L. Jiang, H. Li, J. X. Zhang, L. N. Zhou, and Y. J. Li, Chem. Electro-Chem. 5 (2018) 3901.
[11] S. García-Rodríguez, S. Rojas, M. A. Peña, J. L. Fierro, S. Baranton, and J. M. Léger, Appl. Catal. B106 (2011) 520.
[12] J. Liu, Z. Li, C. He, R. Fu, D. Wu, and S. Song, Int. J. Hydrogen Energy 36 (2011) 2250.
[13] X. Zhang, D. Li, D. Dong, H. Wang, and P. A. Webley, Mater. Lett. 64 (2010) 1169.
[14] C. Xu, Y. Su, L. Tan, Z. Liu, J. Zhang, S. Chen, and S. P. Jiang, Electrochim. Acta 54 (2009) 6322.
[15] S. García-Rodríguez, F. Somodi, I. Borbáth, J. L. Margitfalvi, M. A. Peña, J. L. Fierro, and S. Rojas, Appl. Catal. B 91 (2009) 83.
[16] X. Zhong, X. Zhang, X. Sun, B. Liu, Y. Kuang, and J. Chen, Chin. J. Chem. 27 (2009) 56.
[17] Y. Peng, L. Li, R. Tao, L. Tan, M. Qiu, and L. Guo, Nano Res. 11 (2018) 3222.
[18] T. Sheng, W. F. Lin, C. Hardacre, and P. Hu, Phys. Chem. Chem. Phys. 16 (2014) 13248.
[19] J. Seweryn, and A. Lewera, J. Power Sources 205(2012) 264.

[20] H. Zhu, Y. Liu, L. Shen, Y. Wei, Z. Guo, H. Wang, K. Han, and Z. Chang, Int. J. Hydrogen Energy 35 (2010) 3125.
[21] A. S. Polo, M. C. Santos, R. F. De Souza, and W. A. Alves, J. Power Sources 196 (2011) 872.
[22] C. Zhai, M. Sun, M. Zhu, K. Zhang, and Y. Du, Int. J. Hydrogen Energy 42 (2017) 5006.
[23] J. Hu, C. Yu, C. Zhai, S. Hu, Y. Wang, N. Fu, L. Zeng, and M. Zhu, Catal. Today 315 (2018) 36.
[24] P. Li, Z. P. Li, and B. H. Liu, J. Power Sources 199 (2012)146.
[25] M. Sun, J. Hu, C. Zhai, M. Zhu, and J. Pan, Electrochim. Acta 245 (2017) 863.
[26] M. Zhu, C. Zhai, M. Sun, Y. Hu, B. Yan, and Y. Du, Appl. Catal. B 203 (2017) 108.
[27] H. Ijadpanah-Saravy, M. Safari, A. Khodadadi-Darban, and A. Rezaei, Anal. Lett. 47 (2014) 1772.
[28] B. Deiminiat, and G. H. Rounaghi, Sens. Actuators B 259 (2018) 133.
[29] Z. R. Marand, N. Shahtahmassebi, M. R. Housaindokht, G. H. Rounaghi, and I. Razavipanah, Electroanalysis 26 (2014) 840.
[30] S. Mizuhashi, C. E. Cordonier, H. Honma, and O. Takai, J. Electrochem. Soc. 162 (2015) D497.
[31] R. B. Kutz, B. Braunschweig, P. Mukherjee, R. L. Behrens, D. D. Dlott, and A. Wieckowski, J. Catal. 278 (2011) 181.
[32] L. Zhang, and F. Li, App. Clay. Sci. 50 (2010) 64.
[33] N. Fujiwara, K. A. Friedrich, and U. Stimming, J. Electroanal. Chem. 472 (1999) 120.
[34] M. H. Shao, and R. R. Adzic, Electrochim Acta 50 (2005) 2415
[35] K. D. Snell, and A. G. Keenan, Electrochim Acta 27 (1982) 1631.
[36] H. Wang, Z. Jusys, and R. J. Behm, J Power Sources 154 (2006) 351.
[37] T. Iwasita, and E. A. Pastor, Electrochim. Acta 39 (1994) 531.
[38] Z. Xu, J. Yu, and G. Liu, Electrochem. Commun. 13 (2011) 1260.
[39] Z. Jin, Q. Wang, W. Zheng, and X. Cui, ACS Appl. Mater. Interfaces 8 (2016) 5273.
[40] J. Hu, C. Zhai, H. Gao, L. Zeng, Y. Du, and M. Zhu, Energy Fuels 3 (2019) 439.
[41] J. Lu, S. Lu, D. Wang, M. Yang, Z. Liu, C. Xu, and S. P. Jiang, Electrochim. Acta 54 (2009) 5486.
[42] Z. Liu and L. Hong, J. Appl. Electrochem. 37 (2007) 505.